TRAPPED NOBLE GASES IN THIRTEEN UREILITES FROM ANTARCTICA. K. Nagao[1], M. K. Haba[1], J. Park[2,3], and G. F. Herzog[2], [1]Geochemical Research Center, Graduate School of Science, University of Tokyo, Bunkyo-ku, Tokyo 113-0033, Japan (nagao@eqchem.s.u-tokyo.ac.jp), [2]Department of Chemistry and Chemical Biology, Rutgers University, Piscataway, NJ 08854, USA (jp975@rci.rutgers.edu), [3]Lunar & Planetary Institute, Houston, TX 77058, USA.

Introduction: Ureilites are know to have high concentrations of trapped noble gases, and their host phases are thought to be carbonaceous materials such as amorphous carbon, graphite and diamond [e.g., 1-4]. The origin and trapping mechanism of the trapped noble gases in ureilites, however, are still under discussion. As a part of noble gas study on 13 ureilites from Antarctica [5], we present isotopic compositions of trappted noble gases.

Samples and experimental procedure: Noble gases were measured for bulk samples from 13 different ureilites as shown in Table 1. For two ureilites, GRA95205 and GRA98032, two chips from each meteorite were measured. A noble gas mass spectrometer, modified-VG5400/MS-3, at the University of Tokyo was used for noble gas analysis. Fifteen bulk samples weighing ca. 30–50 mg were installed in a sample holder connected to a noble gas extraction furnace, and then preheated at 150°C overnight in ultra high vacuum condition to remove atmospheric noble gas contamination. Noble gases were extracted by heating each sample in the furnace at 1800°C for 30 min, and then purified with two Ti-Zr getters kept at the temperature of 800°C and SAES-getters (NP-10). The purified noble gases were separeated from eath other before introducing each noble gas (He, Ne, Ar, Kr, and Xe) into the mass spectrometer.

Results and discussion:

Light noble gases. Based on the light noble gas compositions obtained in this work, three different pairs have been identified [5]; 1) ALH82106, ALH82130, and ALH84136, 2) EET87517 and EET87720, and 3) GRA95205 and GRA98032. Cosmic-ray exposure ages for the ureilites are presented in [5]. Although cosmogenic Ne is dominant in the samples, only one ureilite, GRO95575, shows relatively high $^{20}Ne/^{22}Ne$ ratio of 4.3 and indicates a presence of trapped Ne with $^{20}Ne/^{22}Ne$ ratio in a rage from 10 to 11. The ratio agrees with the value of trapped Ne for ureilites, e.g., $^{20}Ne/^{22}Ne$ = 10.5 and $^{21}Ne/^{22}Ne$ = 0.032 [1] and $^{20}Ne/^{22}Ne = 10.7$ (for $0.03 \le {}^{21}Ne/^{22}Ne \le 0.05$) [2].

Ar isotopic ratios. Low $^{40}Ar/^{36}Ar_{trap}$ ratios, 0.05–5.0, are observed for the ureilites. Because of the high concentrations of trapped ^{36}Ar in the range from 6×10^{-8} ccSTP/g (MET01083) to 1.34×10^{-5} ccSTP/g (GRO95575), subtraction of cosmogenic Ar from the measured ^{36}Ar concentrations result in minor corrections in the $^{40}Ar/^{36}Ar_{trap}$ ratios. A plot of $^{40}Ar/^{36}Ar_{trap}$ against $1/^{36}Ar_{trap}$ (Fig. 1) shows that $^{40}Ar/^{36}Ar$ ratio originally trapped in ureiltes was very low, in agreement with the reported low $^{40}Ar/^{36}Ar$ ratios for ureilites; $^{40}Ar/^{36}Ar = (2.9 \pm 1.7) \times 10^{-4}$ was reported for Dyalpur [2]. The apparent increase in $^{40}Ar/^{36}Ar$ with lower concentration of trapped ^{36}Ar could be an incresing contamination of atmospheric Ar to the samples.

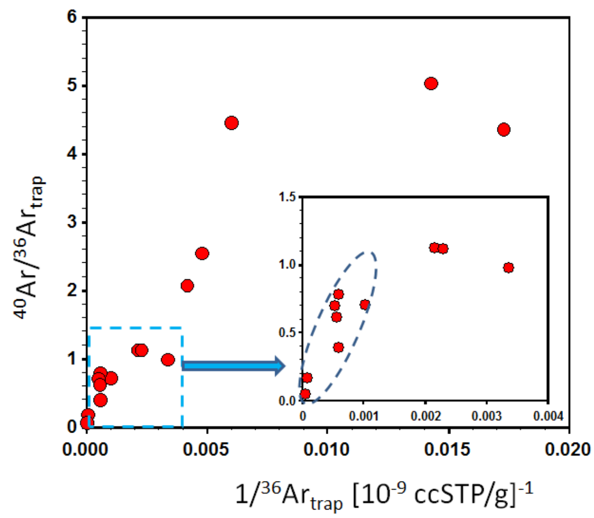

Fig. 1. Plot of $^{40}Ar/^{36}Ar_{trap}$ vs. $1/^{36}Ar_{trap}$. The area for low $^{40}Ar/^{36}Ar_{trap}$ is expanded in the figure.

Abundance ratios of Ar, Kr and Xe. Ratios of $^{36}Ar_{trap}/^{132}Xe$ are plotted against $^{84}Kr/^{132}Xe$ in Fig. 2, where the abundance ratios for Q-gas, a main trapped component in chondrites especially in carbonaceous chondrites, are shown. Positive correlation among the abundance ratios is in good agreement with the reported correlation [e.g., 2, 3], although the spread for our data is narrower and extends to lower plotted area compared with those in [2, 3]. The positive correlation is explained as a selective loss of lighter noble gases Ar and Kr than Xe, resulted in low Ar/Xe and Kr/Xe ratios [2, 3]. The very low $^{84}Kr/^{132}Xe$ ratios, < 0.2, observed for the paired ureilites, ALH82106, ALH82130 and ALH84136, might have been caused by intensive degassing.

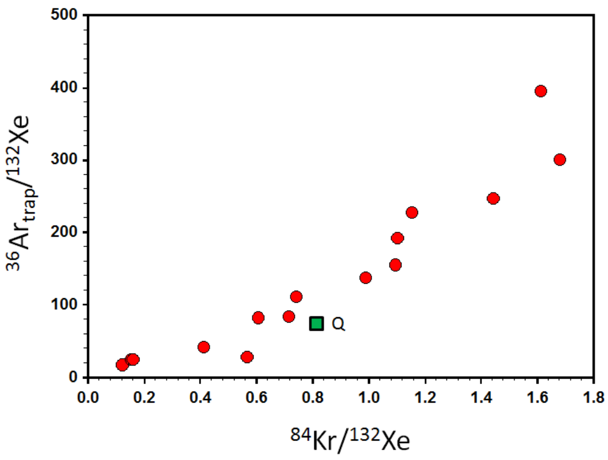

Fig. 2. Trapped ^{36}Ar/^{132}Xe vs. ^{84}Kr/^{132}Xe.

Isotopic compositions of Xe. Isotopic compositions of Xe and ^{132}Xe concentrations for the ureilites are presented in Table 1. Although the isotopic ratios are similar to those of Q-Xe, small differences in some isotope ratios are observed. Fig. 3 shows a plot of ^{130}Xe/^{132}Xe vs. ^{136}Xe/^{132}Xe, where addition of HL-Xe and fissiogenic Xe from ^{244}Pu to Q-Xe is indicated. Data points seem to plot between Q-Xe and solar wind (SW)-Xe. Contribution from HL-Xe or fission-Xe to the trapped Xe is not observed, because of the abundant trapped Q-like Xe in the samples. The data points seem to plot along a mass fractionaton trend from SW-Xe, which may be consistent with the loss of lighter noble gases as indicated in Fig. 2.

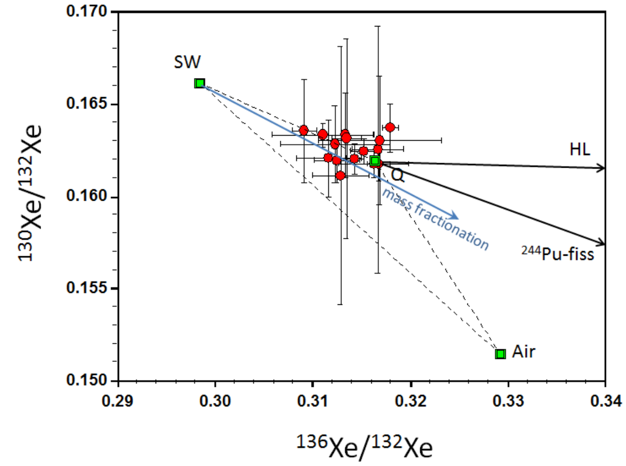

Fig. 3. ^{130}Xe/^{132}Xe ratos are plotted against ^{136}Xe/^{132}Xe ratios. Mixing lines between Q-Xe and HL-Xe, and Q-Xe and Xe produced by fission of ^{244}Pu are shown.

References: [1] Wacker J. F. (1986) *GCA, 50,* 633–642. [2] Göbel R. et al. (1978) *JGR, 83,* 855–867. [3] Okazaki R. et al. (2003) MAPS 38, 767–781. [4] Cosarinsky M. et al. (2010) *41st LPSC,* Abstract #1770. [5] Park J. et al. (2014) *45th LPSC,* Abstract (submitted).

Table 1. Concentrations of ^{132}Xe and Xe isotopic ratios in ureilites from Antarctica.

Sample	^{132}Xe [10^{-12}cc/g]	^{124}Xe/^{132}Xe	^{126}Xe/^{132}Xe	^{128}Xe/^{132}Xe	^{129}Xe/^{132}Xe	^{130}Xe/^{132}Xe	^{131}Xe/^{132}Xe	^{134}Xe/^{132}Xe	^{136}Xe/^{132}Xe
ALH82106-23	14480	0.00445	0.00401	0.0815	1.0428	0.1617	0.8199	0.3791	0.3168
	± 1448	± 0.00003	± 0.00005	± 0.0003	± 0.0038	± 0.0010	± 0.0033	± 0.0008	± 0.0012
ALH82130-35	18807	0.00440	0.00403	0.0817	1.0407	0.1637	0.8201	0.3806	0.3180
	± 1881	± 0.00004	± 0.00004	± 0.0003	± 0.0034	± 0.0013	± 0.0013	± 0.0010	± 0.0008
ALH84136-36	18472	0.00443	0.00400	0.0812	1.0363	0.1625	0.8203	0.3805	0.3167
	± 1847	± 0.00010	± 0.00008	± 0.0012	± 0.0081	± 0.0067	± 0.0067	± 0.0024	± 0.0026
EET83225-30	840	0.00426	0.00395	0.0824	1.0438	0.1620	0.8209	0.3755	0.3117
	± 84	± 0.00032	± 0.00028	± 0.0017	± 0.0049	± 0.0021	± 0.0048	± 0.0033	± 0.0033
EET83309-38	78689	0.00436	0.00409	0.0816	1.0383	0.1620	0.8196	0.3778	0.3144
	± 7869	± 0.00008	± 0.00008	± 0.0006	± 0.0059	± 0.0009	± 0.0016	± 0.0013	± 0.0009
EET87511-32	10634	0.00444	0.00411	0.0817	1.0397	0.1633	0.8195	0.3776	0.3134
	± 1064	± 0.00005	± 0.00006	± 0.0017	± 0.0191	± 0.0023	± 0.0057	± 0.0019	± 0.0028
EET87517-32	2681	0.00447	0.00405	0.0818	1.0511	0.1631	0.8216	0.3781	0.3135
	± 268	± 0.00010	± 0.00009	± 0.0060	± 0.0005	± 0.0054	± 0.0054	± 0.0026	± 0.0015
EET87720-26	2540	0.00419	0.00398	0.0808	1.0399	0.1635	0.8229	0.3755	0.3092
	± 254	± 0.00008	± 0.00013	± 0.0007	± 0.0065	± 0.0028	± 0.0117	± 0.0016	± 0.0013
GRA95205-32	3900	0.00447	0.00401	0.0806	1.0320	0.1611	0.8202	0.3781	0.3129
	± 390	± 0.00010	± 0.00007	± 0.0007	± 0.0160	± 0.0070	± 0.0070	± 0.0027	± 0.0029
GRA95205-33	7214	0.00433	0.00405	0.0807	1.0370	0.1633	0.8201	0.3736	0.3111
	± 722	± 0.00011	± 0.00012	± 0.0014	± 0.0200	± 0.0007	± 0.0078	± 0.0063	± 0.0052
GRA98032-17	9579	0.00439	0.00410	0.0827	1.0360	0.1630	0.8197	0.3802	0.3169
	± 958	± 0.00014	± 0.00013	± 0.0015	± 0.0049	± 0.0035	± 0.0011	± 0.0044	± 0.0063
GRA98032-19	5701	0.00433	0.00399	0.0810	1.0304	0.1619	0.8228	0.3768	0.3125
	± 570	± 0.00012	± 0.00008	± 0.0005	± 0.0038	± 0.0012	± 0.0036	± 0.0015	± 0.0023
GRO95575-17	34952	0.00438	0.00408	0.0818	1.0424	0.1628	0.8236	0.3778	0.3123
	± 3495	± 0.00015	± 0.00011	± 0.0015	± 0.0223	± 0.0021	± 0.0087	± 0.0053	± 0.0056
MET1083-5	1416	0.00431	0.00407	0.0816	1.0393	0.1617	0.8206	0.3810	0.3163
	± 142	± 0.00020	± 0.00028	± 0.0008	± 0.0050	± 0.0008	± 0.0029	± 0.0042	± 0.0036
MET1085-5	6058	0.00442	0.00411	0.0815	1.0430	0.1624	0.8220	0.3794	0.3153
	± 606	± 0.00010	± 0.00006	± 0.0012	± 0.0079	± 0.0007	± 0.0029	± 0.0013	± 0.0014